Structural Stability for AR Guided Construction

Vittorio Paris(✉) and Davide Prati

Department of Engineering and Applied Sciences, University of Bergamo, Via G. Marconi 3, Dalmine, BG, Italy
vittorio.paris@unibg.it

Abstract. Numerous installations, i.e., Armadillo project, Angelus Novus, or InnixAR, demonstrate a renewed interest in masonry constructions. Despite efforts, the application of arches, vaults, and domes in current construction practices remains limited. High construction costs and limited knowledge in construction are among the reasons for their limited contemporary use. The study and the application of the scaffold-free vaulting techniques highlight even more complications. Several investigations focus on combining the potential of digital tools, such as AR technologies, with innovative design approaches to overcome existing challenges. AR could facilitate complex tasks, impact the learning curve, and provide a relevant aid in tracing operations. The research investigation focuses on demonstrating that deep control over structural investigation could support design choices and provide valuable information for using AR.

Keywords: Distinct Element Method · Augmented reality · Thin tile vaulting

1 Introduction

1.1 Research Context

The Architecture, Engineering, and Construction (AEC) sector has undergone a profound transformation since the late twentieth century, characterised by increasing specialisation of roles and progressive mechanisation of construction processes [15]. While these developments have improved efficiency in contemporary building processes, they have also resulted in a highly fragmented production chain, where coordination and management have become critical yet complex tasks [4].

The transition towards digitalisation, accelerated by the introduction of Building Information Modelling (BIM) standards such as the ISO 19650 series, has further increased the level of process integration required across design and construction phases. Within this evolving framework, the reconstruction and construction of masonry arches and vaults reveal criticalities. Unlike contemporary structural systems based on reinforced concrete or steel, masonry vaults are governed by geometry-dependent equilibrium conditions [12], requiring a high level of craftsmanship and an implicit understanding of structural behaviour [5]. These limitations are exacerbated in renovation and heritage contexts, where interventions must account for the non-standard geometry of

© The Author(s), under exclusive license to Springer Nature Switzerland AG 2027
O. Gervasi et al. (Eds.): ICCSA 2026 Workshops, LNCS 16758, pp. 551–563, 2027.
https://doi.org/10.1007/978-3-032-30497-1_33

historical buildings, are subject to limited accessibility, and are characterised by high uncertainty.

A further critical issue is the erosion of traditional construction knowledge, particularly in highly skilled roles [7]. In the case of historical scaffold-free vaulting techniques,e.g., Thin-Tile (TT) vaulting [10], the shortage of skilled labour [7] severely hinders the development of a new generation of masons capable of applying such advanced construction techniques. Indeed, all scaffold-free vaulting methods, such as herringbone or TT vaulting, require many years of apprenticeship, during which the mason learns the secrets of these construction techniques through practice. A lack of knowledge of how to apply scaffold-free vaulting methods affects quality and productivity. It directly affects structural safety during construction, as geometric deviations can significantly alter load paths and stability, necessitating external temporary supports (Fig. 1).



Source: Eurostat [ei_bsin_q_r2; ei_bsbu_m_r2; ei_bsse_q_r2; une_rt_m]

Fig. 1. Resume of labour shortage vs unemployment rate in the AEC sector for European countries [7].

1.2 Notes on AR as a Tool for Supporting the Construction Phase

Digital technologies, such as robotics and additive manufacturing, although promising, are not yet integrated into on-site processes; they cannot replace human behaviour in on-site construction. Many operations are still performed without digital support, leading to inefficiencies, information loss, and increased variability in execution. Among emerging technologies capable of bridging the gap between design and construction phases, unmanned aerial vehicles and Augmented Reality (AR) have attracted increasing attention. Unmanned aerial vehicles are widely used nowadays for surveying and monitoring, and provide valuable support in open environments or during the preliminary phase of design.

AR has the potential to integrate digital information directly into the physical construction environment. It enables the superimposition of georeferenced digital content onto real-world contexts, offering new possibilities for supporting on-site decision-making, geometric control, and workflow coordination. Several studies have predominantly focused on the use of AR in construction management, addressing issues related

to supervision [3], performance monitoring, and safety [1]. The construction phase is the most critical yet least efficient stage of the process, as it entails the direct materialisation of the design through the coordinated actions of multiple actors, including engineers, architects, and skilled workers. In this context, AR has demonstrated potential in improving communication, coordination, and quality control. By leveraging Building information models, AR systems enable real-time design review, clash detection, and visualisation of construction sequences, thereby enhancing the understanding of complex assemblies. AR can assist in tracing geometries, controlling the positioning of individual elements, and ensuring adherence to predefined construction logic. Furthermore, AR-based systems can enhance safety by identifying potential hazards and communicating risk information directly to workers through wearable devices, thus enabling proactive risk management.

Despite the promising capabilities, the application of AR within the AEC sector remains limited. AR technologies are still evolving; the absence of shared standards limits their maturity, as well as the availability of consolidated methodological frameworks and hardware.

1.3 Technology Application of Augmented Reality for REnovation Work (TAARReW) Research

The paper reports the design methodology for defining the case study, and the partial findings of the construction approach adopted in the Technology Application of Augmented Reality for REnovation Work (TAARReW) project. TAARReW aims to assess the potential impact of AR in the construction of complex masonry structures. The research proposes a preliminary methodology for designing the assembly process that accounts for structural considerations. In the research, a specific technique was investigated: the TT vaulting, a historical, scaffold-free technique that utilises gypsum-based mortar and lightweight, thin tiles [10]. TT vaults are environmentally sustainable, light, and stiff structures [2]. Like all shells, they can withstand tremendous loads with a modest amount of material [2]. Unlike other curved structures, their construction does not require temporary supports, avoiding the need to build centering and reducing waste [11]. However, mastering the TT vaulting technique requires several years of training, and, due to the lack of trained labour, only a few master masons can apply it properly nowadays. The preservation of techniques such as TT is essential for safeguarding historical masonry shells. One of the most challenging tasks in TT techniques is tracing curved geometry in the air. To this end, the AR supported tracing by projecting the shell geometry at the exact position and providing step-by-step guidance and real-time instructions, thereby facilitating on-site construction operations.

2 Methodology

2.1 Design of the Case Study

To evaluate the design of the assembly process, a TT Lowered Vault (LV) was geometrically designed as a case study. The LV measures 1.4 × 1.4 m, with a rectangular base and is composed of more than 50 thin tiles forming the patterning shown in Fig. 2. The

vault rise is about 15 cm, i.e., the ratio of rise to span is about 0.11. The adopted tile dimensions are approximately 3.5 × 12 × 25 cm, and it weighs 1.4 kg, while the mortar joints are approximately 1 cm thick.

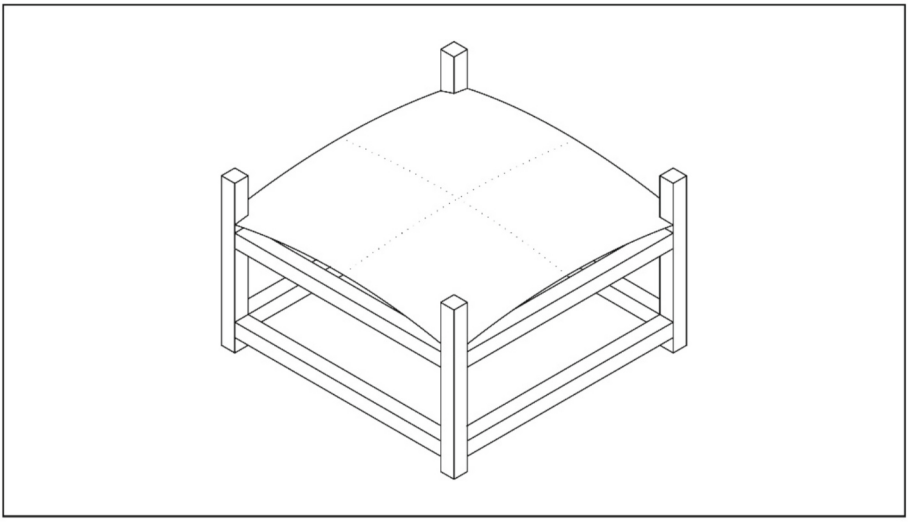

Fig. 2. Design of the lowered vault.

The overall LV design was defined, taking into account the existing literature [14], practical experience, and interviews with master masons, and aimed to highlight the characteristics of the TT technique. Two patterns (A) and (B) were evaluated. As depicted in Fig. 3, the (A) tiling pattern is a spiral, with tiles arranged to start from the center toward the edges of the shells. The tiles of the (B) were placed parallel to one another, forming several arches with the same span and different rises, see Fig. 4. For both, the structural state during construction was evaluated to assess the feasibility of safe construction.

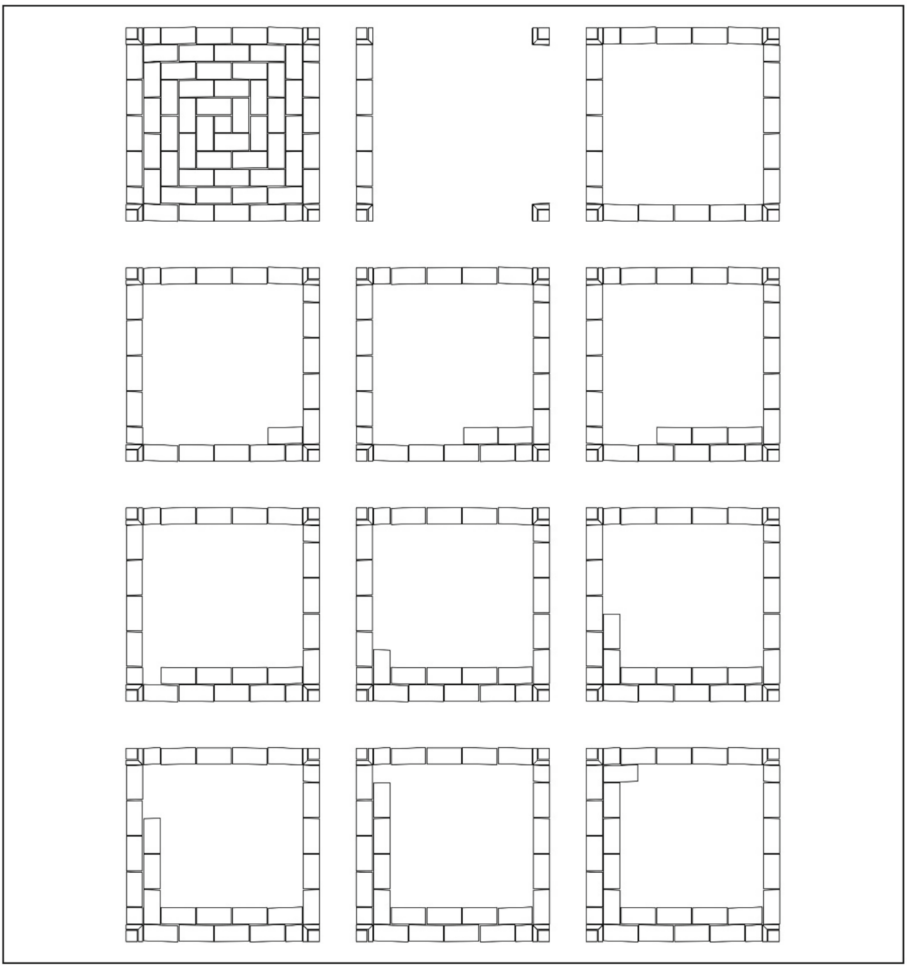

Fig. 3. Top view of the (A) pattern of the LV (Top-left). Scheme of the construction sequence (from top to bottom).

The construction sequences accounted for (A) consisted of following the spiral geometry and laying the 61 tiles to build 20 arches sequentially. These arches are classified as sub-structures. The first four arches built are the ones near the edge of the LV with maximum span, while the last tile corresponds to the central element positioned at t the crown of the vault. The arches present decreasing spans; the first four arches laid have a thickness-above-span ratio of 0.025, while the inner arches have a ratio of 0.095. The average thickness-above-span ratio is 0.048.

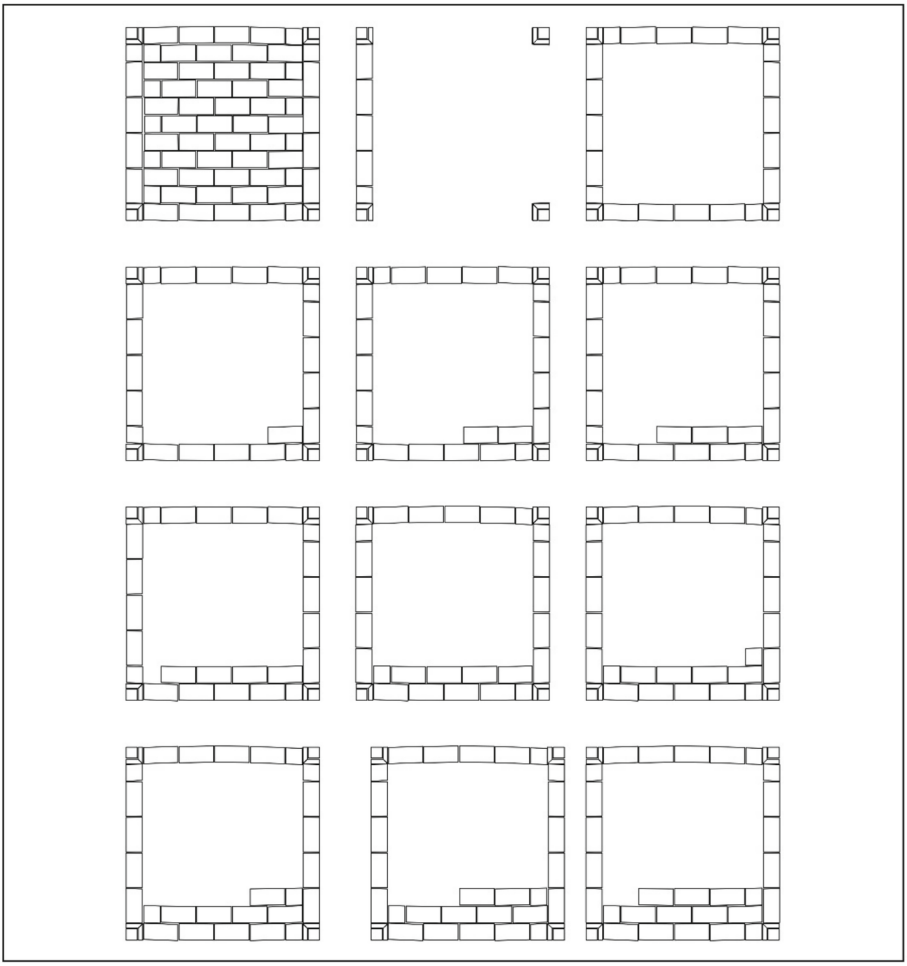

Fig. 4. Top view of the (B) pattern of the LV (Top-left). Scheme of the construction sequence (from top to bottom).

The (B) pattern instead presents arches with a constant span with a thickness-above-span ratio of 0.025. Here, the simulated construction sequence consists of laying the four external arches as shown in Fig. 4, and then placing the tiles to create parallel arches. For both patterns, the four external arches were built using centering; hence, the structural state was simulated once closed. For both LV patterns, the mortar joints were designed to be 0.5–1.0 cm thick, and no on-site tile cutting was allowed.

The (A) pattern was designed based on the TT traditional pattern, while the (B) pattern is not commonly used.

2.2 The Numerical Model

Two sets of structural analyses were performed: one assuming a Construction with Centering (CC) and the other simulating the Construction adopting the TT (CTT) techniques (b). The CC was conducted to evaluate the overall state of both patterns (A) and (B). Once the overall structural state was established, the CTT aimed to highlight the feasibility and impact of construction techniques on structural behaviour. Both CC and CTT analyses were carried out using numerical simulations with the Distinct Element Method (DEM) [6] in 3DEC 9.0 (Itasca, Minneapolis, MN, USA) [8].

The LV was described as a system of rigid bodies, in which each body is a thin tile, and, unlike other numerical methods [9], the bodies can slide, rotate, collide, or even detach from one another. The evolution of the system of rigid bodies is carried out by the explicit integration of Newton's laws of motion.

Deformable joints are modelled at the interfaces between bodies. The interfaces, tile-mortar-tile, were modelled using a spring system governed by the Mohr-Coulomb friction model with a tensile cutoff. The normal (jK_N) and the shear (jK_S) stiffness of the springs are defined by (1) and (2) [13]:

$$jK_N = \frac{E_m E_t}{l_m E_t + l_t E_m} \tag{1}$$

$$jK_s = jK_N 10^{-1} \tag{2}$$

where E denotes the Young modulus, l corresponds to the characteristic dimension of the brick, and the subscripts t and m indicate the tile and mortar, respectively. Deformations and displacements of the actual structures are lumped at the interfaces.

The values of Em and Et were obtained from the datasheet and the literature [x], accounting for the setting phenomena in Em estimation. The adopted Et value is about 3.4·1010 Pa, while Em is about 2·109 Pa after mortar hardening (i.e., for the CC analyses). For CTT simulations, the value was determined through physical testing. The jKN values range from 8·1010 Pa/m to 1.94·1011 Pa/m for CCT and CC, respectively.

Precisely as for jKN and jKS, the values of j_{ten} and j_{coh} were evaluated at different curing ages, assuming a tensile cut-off equal to the cohesion value for safety. For CTT numerical analyses, $j_{ten} = 2.5{\cdot}10^{10}$ Pa and j_{coh} $2.5{\cdot}10^{10}$ Pa [11]. The friction angle is equal to 33°. All numerical analyses were performed under self-weight only, assuming fixed blocks at the corners.

3 Results

3.1 CC Simulations

The CC numerical analyses carried out on LV (A) and (B) underline the similar behaviour. The maximum displacement is $2.35{\cdot}10^{-2}$ mm recorded in (B), while (A) displays a maximum of $2.13{\cdot}10^{-2}$ mm. The displacement maps shown in Fig. 5 indicate negligible differences attributable to TT patterns. (A) LV shows a wider area with displacement above $2.00{\cdot}10^{-2}$ mm. Due to the modest dimension of the LV, the stresses are extremely low.

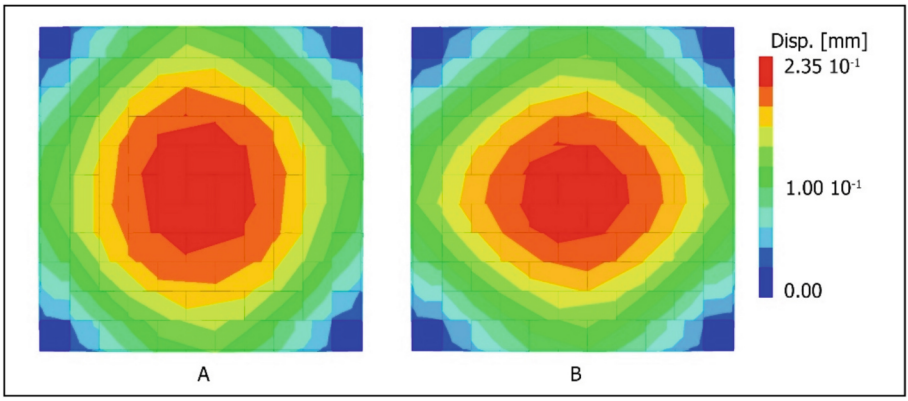

Fig. 5. Top view of the displacement map of (A) and (B) LV, CC simulations.

3.2 CTT Simulations

As mentioned in Sect. 2, CTT was carried out by investigating the possibility of building without the need for centering adopting the TT vaulting technique. The construction was divided into sequential steps, and for each step, the structural evaluation was executed. The first four steps correspond to the construction of the four external arches, because they had to be built with centering. After those for each tile, a new step was implemented, and the structural state was numerically assessed. For both LV (A and B), the displacement of the X checkpoints was recorded to observe the local response of the vault. In practice, the equilibrium of the tile during laying depends on the mortar's material properties: traditionally, Gypsum mortar is used, and the maximum weight of each tile should be less than 1.4 kg. Each thin tile weighs 1.2 kg.

The LV characterised by (A) pattern is stable, with no collapse or local failure. The displacement map changes drastically compared with the CC analyses. During the construction of the four external arches, the maximum displacements are about 0.1 mm, located near the central portion of each arch. The CCT simulations show that, once built, the arches remain stable until the inner tiles are laid. Then, the vertical displacements increase. Upon completion of construction, the maximum displacements of the external arches reach about 0.4 mm.

The CCT simulation highlighted the impact of constructing without temporary supports. During construction, the completed arches already in place provide the resources to avoid collapse, balancing the out-of-plane loads from the new inner tiles being laid. This out-of-plane displacement is visible in the displacement map shown in Fig. 6 for the (A) pattern. On the other hand, the numerical simulation of the (B) pattern shows the role of the tiling pattern and substructures in structural stability. The numerical simulation associated with (B) was conducted using the same approach as in (A). The external arches were built with external support, then the vaulting sequence continued as depicted in Fig. 4. The simulation underscores the instability of such a construction sequence. During the first steps, the behaviour of the first four arches is the same as in the (A) case, then when the second inner arch is laid, collapse occurs, see Fig. 7.

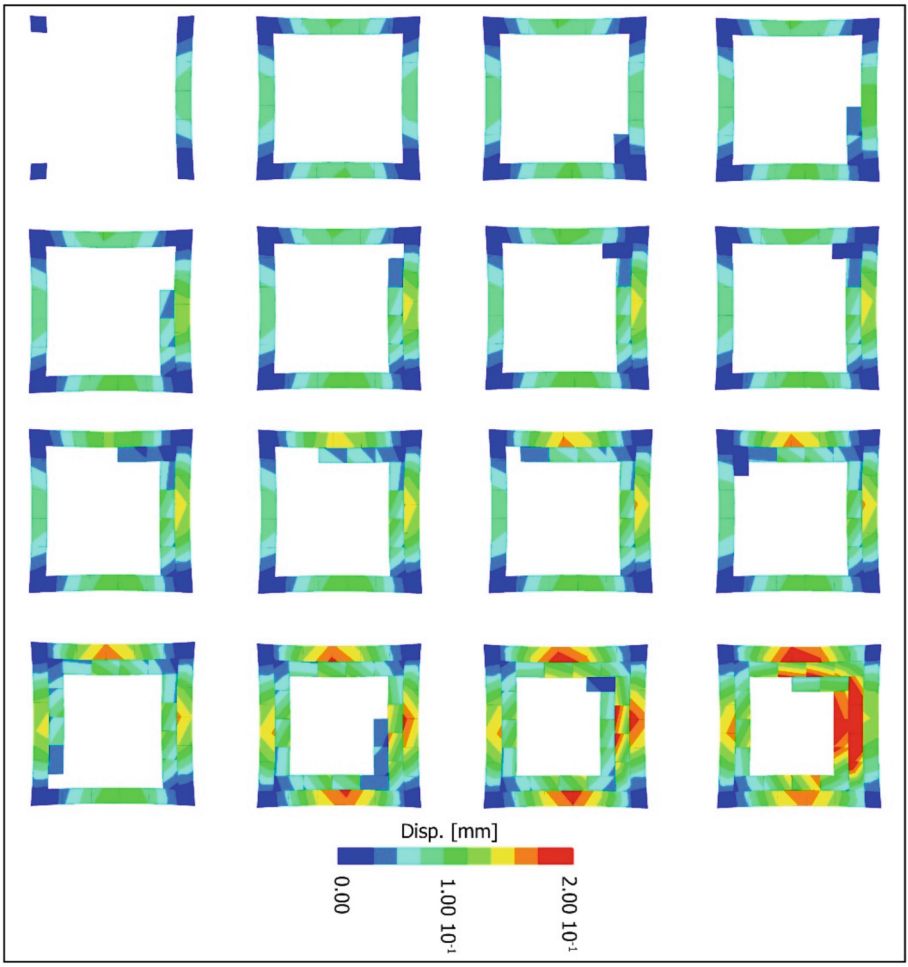

Fig. 6. Top view of displacement maps of (A) LV, CTT simulations. Starting from the top left and moving toward the bottom right, each row shows the variation in displacement according to the traditional construction sequence.

The different construction sequence affects the structural stability, drastically impacting the equilibrium. The numerical analyses show slipping at the interface between the second and third inner arches due to tensile failure. Regarding the (B) pattern, further investigation was conducted to account for the sensitivity of j_{ten} and j_{coh}. The equilibrated state was found when j_{ten} and j_{coh} were assumed equal to $6{\cdot}10^{10}$ Pa.

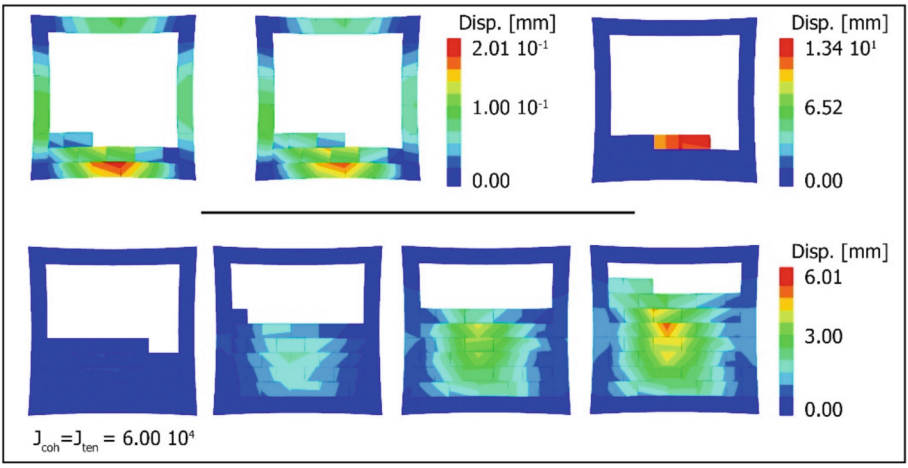

Fig. 7. Top view of displacement maps of (B) LV, CTT simulations. In the top row j_{ten} and j_{coh} equal to CCT simulation for (A) pattern. In the bottom row, the values of jten and jcoh were assumed to be more than 2 times the CCT simulation values for the (A) pattern.

3.3 The Physical Tests

The (A) model was built by a team of masons with no prior experience in vaulting, aided by AR systems. The AR supports the mason with the tracing operation. The team attended a 2-h workshop on AR and was trained in the TT vaulting technique, using standard training. i.e., tutorials, videos, audio testimonies, and manuals. The team tested the framework developed within the TAARReW. It aimed to integrate AR into the construction process as an operative system for real-time guidance and control, explicitly grounded in structural stability criteria. The approach departs from conventional AR applications limited to visualisation, and instead defines a process-driven workflow in which digital projections are generated according to both geometric and structural requirements. The very same construction sequence modelled for numerical analyses was implemented to enrich with information related to the construction sequence, which is treated as a critical parameter for the knowledge transfer.

Unlike traditional approaches, which verify stability primarily in the completed structure, this methodology explicitly accounts for the evolution of stability during construction. Based on the decomposition performed for CTT simulations, the AR system is configured to project tracing lines and positioning guides from the digital model. During the on-site construction phase, operators use AR devices (e.g., head-mounted displays or handheld devices) to visualise the projected tracing lines directly within the physical environment. Each element is manually positioned according to these projections, which indicate not only its location but also its orientation, its relation to adjacent units, and the correct sequence of construction.

Upon completion, a geometric validation was conducted by comparing the as-built structure with the original design model. This enables assessment of deviations and evaluation of the effectiveness of the AR-guided process in maintaining structural fidelity.

Overall, the proposed methodology establishes a deep relationship among design, construction, and structural behaviour, with AR serving as an interface between digital information and manual execution. The workflow enables the construction of complex geometries with enhanced accuracy, reduced reliance on formwork, and improved stability control throughout the entire building process.

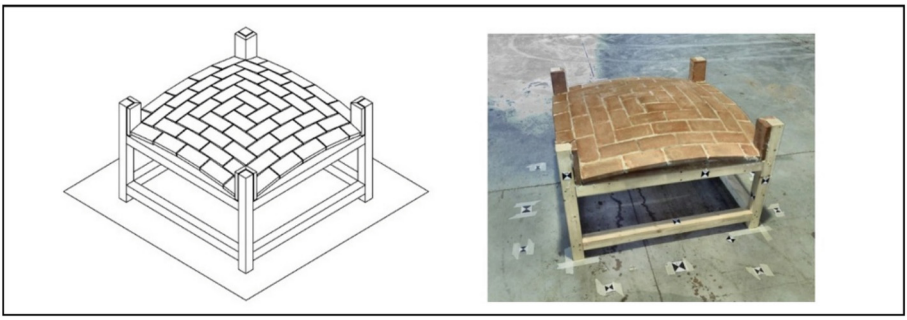

Fig. 8. Lowered vault built by T2, employing AR.

A survey using a laser scanner was conducted to assess the vault's accuracy in comparison to the digital model. The parameters were selected to ensure a survey with sufficient accuracy and precision, enabling evaluation of geometric deviations from the designed model. The scanning was performed with a resolution of 3 mm at distances beyond 10 m, a quality setting of 3X, and a reduced field of view ranging from 60° to 0° in the vertical plane and from 140° to 240° in the horizontal plane. The scan duration was reduced to 8 min and 34 s, enabling detection of both the RGB channel and the reflectance threshold. Back-office alignment was performed using both sets of markers, with those placed on each vault, to obtain accurate alignments. Mean errors on targets were also confirmed by evaluating scan statistics on individual points. Overall, based on approximately 48 million points surveyed, the average error was 1.4 mm, with a maximum of 1.7 mm and a minimum scan overlap of 32.6%.

The comparison between the point clouds and the designed geometry was carried out using Cloud Compare software, and it reveals the geometrical discrepancies. Indeed, the colour map of the geometrical discrepancy shown in Fig. 8 displays a range of −1.4 to + 3.0 cm. Positive values in the range indicate that the measured points lie above the designed geometry, whereas negative values indicate points below it (Fig. 9).

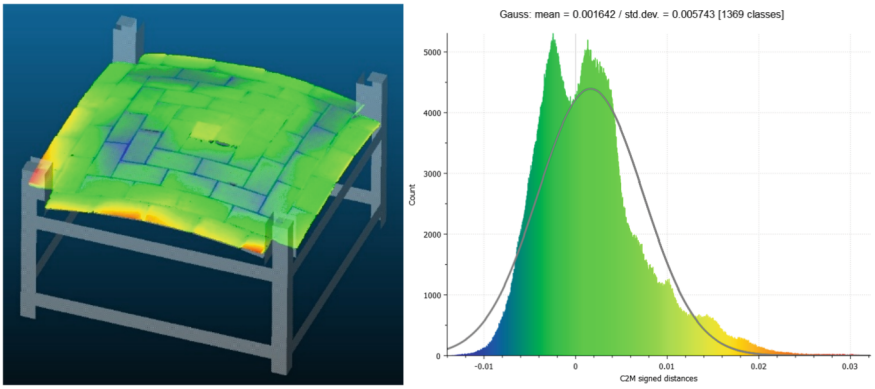

Fig. 9. Comparison of built model vs designed geometry. Left: geometrical discrepancy colour map. Right: distribution of geometrical discrepancies

4 Discussion

The research explored the integration of AR, parametric design, and historically grounded self-balanced construction principles to support the preservation of efficient scaffold- free vaulting techniques. The study uses AR-assisted guidance to execute geometrically complex tasks, thereby improving spatial accuracy and reducing dependence on highly specialised craftsmanship.

The numerical results indicate that the proposed workflow for DEM simulation has the potential to address several critical limitations that currently hinder the adoption of masonry vaulting systems. By incorporating the construction sequence into structural assessment and integrating it with AR tools, it is possible to overcome a lack of practical knowledge.

However, the present study represents an initial step within a broader experimental framework. Future work will focus on extending the validation of the proposed methodology through additional empirical testing. In particular, further analyses will be conducted to validate the CCT simulation associated with the(B) pattern. Moreover, additional tests will be completed to deepen the evaluation of performance metrics, including geometric accuracy, construction time, cognitive load, and overall process efficiency.

These forthcoming investigations will help consolidate the methodological framework and define operational best practices for implementing AR-assisted masonry construction in both experimental and real-world applications.

Funding. The project was supported by the Young Independent Research Group – CUP F55F21002580006: Technology Application of Augmented Reality for Renovation work (TAAReW) fund.

References

1. Abraham, M., Annunziata, M.: Augmented Reality is already improving worker performance (2017). https://hbr.org/2017/03/augmented-reality-is-already-improving-worker-performance

2. Adriaenssens, S., et al. (eds): Shell structures for architecture: form finding and optimisation. Routledge/Taylor & Francis Group, London ; New York (2014)
3. Alkan, I.B., Basaga, H.B.: Augmented reality technologies in construction project assembly phases. Autom. Constr. **156**, 105107 (2023). https://doi.org/10.1016/j.autcon.2023.105107
4. Barbosa, F. et al.: Reinventing Construction: A Route of Higher Productivity. McKinsey Global Institute (2017)
5. Collins, G.R.: The transfer of thin masonry vaulting from Spain to America. J. Soc. Archit. Hist. **27**(3), 176–201 (1968). https://doi.org/10.2307/988501
6. Cundall, P.A.: Formulation of a three-dimensional distinct element model—Part I. A scheme to detect and represent contacts in a system composed of many polyhedral blocks. Int. J. Rock Mech. Min. Sci. Geomech. Abstracts **25**(3), 107–116 (1988). https://doi.org/10.1016/0148-9062(88)92293-0
7. European Construction Observatory: Analytical report on skills: European Construction Observatory. European Commission (2026)
8. Itasca Consulting Group Inc.: 3DEC (2016). https://www.itascacg.com/software/3dec
9. Meloni, G., et al.: Parametric modelling and nonlinear FE analysis of trepponti bridge subjected to differential settlements. Buildings **16**(1), 47 (2025)
10. Ochsendorf, J.A.: Guastavino Vaulting: The Art of Structural Tile. Princeton Architectural Press, New York (2013)
11. Paris, V., et al.: The impact of construction on the structural design of a complex masonry curved shell. Int. J. Space Struct. **40**(2–3), 180–194 (2025). https://doi.org/10.1177/09560599251381901
12. Pingaro, N., et al.: A numerical strategy to assess the stability of curved masonry structures using a simple nonlinear truss model. Buildings **15**(13), 2226 (2025)
13. Simon, J., Bagi, K.: Discrete element analysis of the minimum thickness of oval masonry domes. Int. J. Arch. Heritage **10**(4), 457–475 (2016). https://doi.org/10.1080/15583058.2014.996921
14. Tablet, M.D.P.: Bóvedas extremeñas y alentejanas de rosca y sin cimbra
15. OECD Skills Outlook 2025: Building the Skills of the 21st Century for All. OECD Publishing, Paris (2025). https://doi.org/10.1787/26163cd3-en